J19.3 EXPERIMENTAL LAMP 2-H CONVECTION GUIDANCE FORECASTS ON A 20-KM GRID

Jerome P. Charba*
Frederick G. Samplatsky
Phillip E. Shafer
Meteorological Development Laboratory
Office of Science and Technology
National Weather Service, NOAA
Silver Spring, Maryland

1. INTRODUCTION

Convective storms continue to pose a major challenge for aviation safety and economics, which could be mitigated through improved prediction. The Meteorological Development Laboratory (MDL) of the National Weather Service (NWS) is addressing the high demand for improved convection prediction by providing probabilistic thunderstorm guidance forecasts with Model Output Statistics (MOS) applications for projections of 12 hours and beyond (Hughes 2004) and with the Localized Aviation MOS Program (LAMP; Charba and Liang 2005a; Charba and Samplatsky 2009) for shorter projections. An important aspect of these guidance forecasts is that a thunderstorm is defined solely on the basis of cloud-to-ground (CTG) lightning strikes as reported by the National Lightning Detection Network (NLDN; Cummins et al. 1998).

The definition of convection used in the Collaborative Convective Forecast Product (CCFP; http://aviationweather.gov/products/ccfp/docs/pdd-ccfp.pdf), a key guidance tool used by the U.S. Federation Aviation Administration, is based on the radar reflectivity of precipitation. Thus, the CTG-lightning-based definition of thunderstorms used in MDL guidance products has limited applicability to aviation forecasting, as some convective storms (especially those associated with tropical systems) contain little or no CTG lightning (Charba and Samplatsky 2009). This limitation is addressed in this study, as a new convection predictand is defined from a combination of radar reflectivity and CTG lightning data.

In addition, an independent assessment of the usefulness of the currently operational LAMP lightning probabilities as aviation forecast guidance to supplement the CCFP (Mahoney et al. 2009) indicated the lightning probabilities exhibited weak skill and sharpness during mid-summer months, particularly for the 1500 UTC LAMP cycle and forecast projections beyond about 6 hours. This deficiency is also addressed here by upgrading the MOS forecast input into LAMP (Ghirardelli and Glahn 2010), as two National Centers for Environmental Prediction (NCEP) operational models (rather than one in the current product; Charba and Liang 2005a) are used. Otherwise, the new convection model is similar to the current lightning model [an overview of the latter is provided by Charba and Samplatsky (2009), which is henceforth referenced as CS].

To date, the basic structure of the LAMP convection model is mature, but some aspects are still evolving and a few components remain to be completed. Thus, the model description, results, and findings presented here are somewhat preliminary and incomplete.

2. CONVECTION PREDICTAND DEFINITION

Convection events over the forecast domain (Fig. 1) are defined from a combination of radar reflectivity measurements from the WSR-88D radar network (Fulton et al. 1998) and CTG lightning strike measurements from the NLDN. The radar data are taken from radar coded messages (RCM; OFCM 1991), wherein reflectivities are coded within 10-km gridboxes for a local sub-grid for each network radar site. These sub-grids are composited to form national grids and the latter are quality controlled (Kitzmiller et al. 2002). Lastly, supplemental quality control is applied to the national grids prior to use in LAMP (Charba and Liang 2005b).

A convection event is defined for a 20-km grid box during a 2-h valid period with two criteria for an occurrence: ≥ 40 dBZ radar reflectivity and/or one or more CTG lightning strikes. A convection non-

* *Corresponding author address:*
Dr. Jerome P. Charba, National Weather Service
1325 East West Highway, Room 10410
Silver Spring, MD 20910-3283
email: jerome.charba@noaa.gov

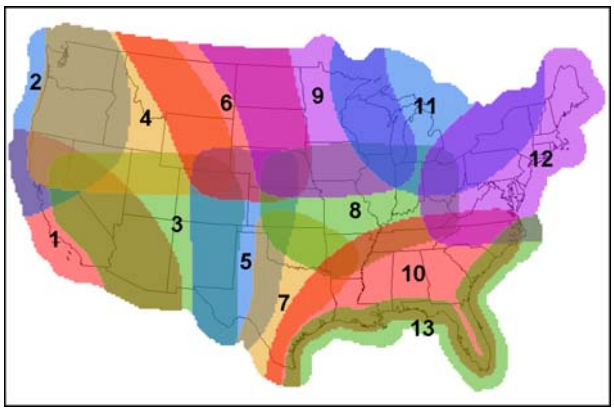

Figure 1. Forecast domain, which is comprised of thirteen overlapping geographical areas (region numbers shown) used for regionalizing the LAMP convection prediction model. The region number is positioned within the non-overlap portion of a given region, and the color shade changes where the region overlaps adjacent regions.

occurrence or occurrence (0 or 1 value) is specified for various combinations of these criteria as shown in Table 1. Note that an entry is not shown where CTG lightning data are missing since extremely rare instances of observational gaps in the lightning data archive are removed from the sample beforehand (Charba and Liang 2005b). Also, for the combination of missing reflectivity data and no CTG lightning, we chose to assign a 0 rather than missing to minimize sample shortening due to missing radar data. This choice should be reasonably safe since much of the missing radar data falls in the mountainous western U.S. (see Figs. 10 and 11 of Charba and Liang 2005b) where warm season convection is highly electrified. Finally, it is important to note that the LAMP lightning predictand mentioned in the Introduction is identical to the convection predictand, except only the lightning criterion in Table 1 is used for the former.

Table 1. Convection predictand values for various combinations of the radar reflectivity and CTG lightning criteria.

≥ 40 dBZ reflect. ?	≥ 1 CTG strikes ?	Predictand value
no	no	0
missing	no	0
missing	yes	1
no	yes	1
yes	no	1
yes	yes	1

3. GFS- AND NAM-BASED MOS CONVECTION PROBABILTY FORECASTS

In accordance with the LAMP framework (Ghirardelli and Glahn 2010), most predictive input from an operational numerical weather prediction (NWP) model is in the form of MOS forecasts for the predictand. Here the MOS input consists of convection probabilities for projections in the 9- to 30-h range from the 0000, 0600, 1200, and 1800 UTC model cycles. For development of the MOS forecasts, archived output from two NCEP NWP models were available: the Global Forecast System (GFS; Kanamitsu et al. 1991) and the North American Mesoscale model (NAM; Rodgers et al. 2005). The historical periods are April 2002 – October 2010 for the GFS and June 2006 – October 2010 for the NAM.

Because the lengths of the GFS and NAM archives were substantially different, separate convection probability regression equations, based on the conventional MOS approach (Glahn and Lowry 1972), were developed from the GFS and NAM model output. Also, separate regression equations were developed where the data for the period October 2009 – October 2010 were withheld to test the performance of the convection probabilities. The MOS equations were stratified according to three "seasons" [16 October – 15 March (cool); 16 March – June 30 (spring); 1 July – 15 October (summer)], and they were "geographically generalized", where a single equation applies to the full CONUS domain (Hughes 2004). The latter "national" approach is efficient computationally, and it avoids the problem of spatial inconsistency in the probabilities at regional boundaries (section 4).

Comparative verification of GFS- and of NAM-based MOS convection probabilities from preliminary regression equations showed the GFS yielded only very slightly better (lower) Brier scores (Brier 1950) and reliability (Wilks 2006) than the NAM (not shown). In this test, these GFS and NAM scores were averaged over the full archives of each model with cross-validation (Wilks 2006), where a full season of data was withheld for individual scores involved in the average. This result suggested the shorter NAM sample could be adequate for developing follow-on "ensemble" MOS convection probability regression equations where the initial, single-model MOS convection probabilities are the sole predictors. Also, comparative inspection of probability maps for selected cases revealed the NAM-based probabilities had much higher spatial detail than the GFS probabilities.

This scale contrast suggested an interactive predictor (Charba and Samplatsky 2011a) computed from the two convection probabilities could provide supplemental predictive information.

Several regression experiments with the GFS and NAM convection probabilities were conducted to investigate these ideas. Specifically, the GFS and NAM probabilities were regressed as separate predictors to produce GFS+NAM MOS "ensemble" convection probability equations. Also, an interactive predictor defined as the simple product of the GFS and NAM probabilities was used together with the initial GFS and NAM probabilities to develop three-predictor "super-ensemble" (SES) convection probability regression equations. Otherwise, the derivation of the two types of ensemble equations was identical to the original GFS and NAM convection probability equations.

To examine the comparative performance of the GFS-, NAM-, GFS+NAM, and SES-based MOS convection probabilities, we computed seasonal Brier skill scores (BSS; Wilks 2006) using the October 2009 – October 2010 independent sample (Fig. 2) where monthly relative frequencies of the convection predictand (section 4) were used as the climatological forecasts. Several findings in Fig. 2 are relevant to this study. (1) GFS-based skill is higher than NAM skill, except at short projections during spring and summer. This result is consistent with the finding of slightly superior GFS performance in the initial comparative verification experiment (discussed above) where cross-validation scoring was used. (2) GFS+NAM skill is substantially better than GFS or NAM skill, which reflects the predictive enhancement of a combined-model MOS approach. (3) SES skill is generally better than GFS+NAM skill (the few projections in Fig. 2 where the SES and GFS+NAM skill is the same may arise from sample shortness). This finding reflects the added predictive contribution of the GFS-NAM probability-product predictor.

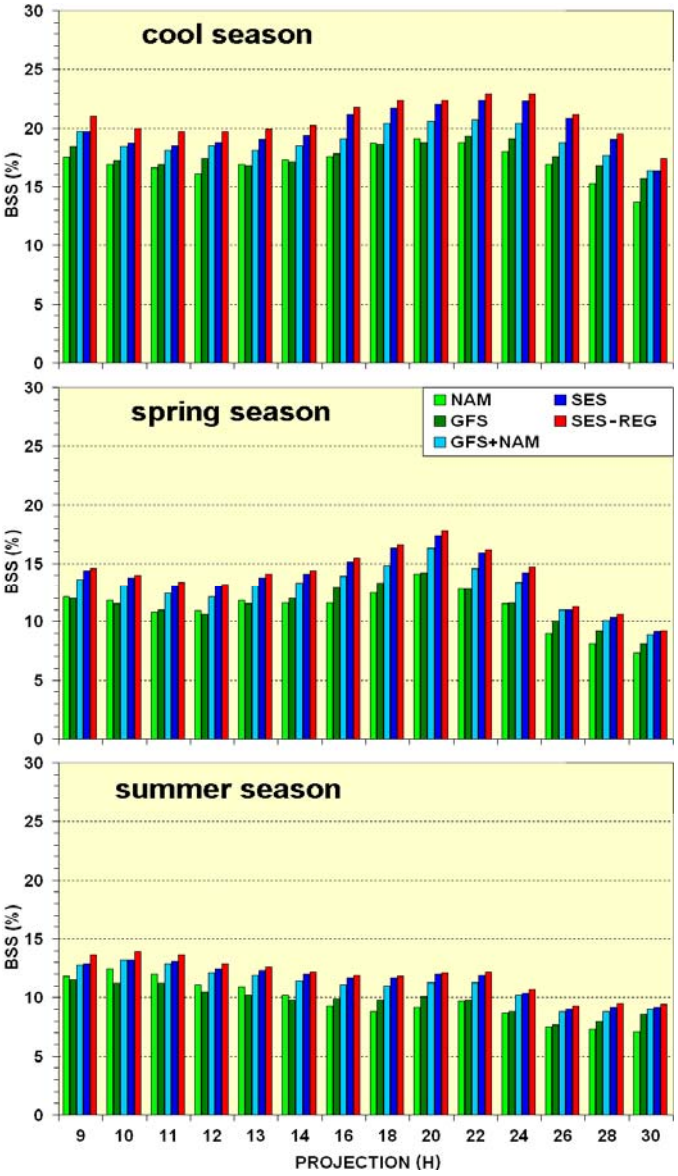

Figure 2. Brier skill score (BSS; %) versus forecast projection (h) from 1200 UTC for various MOS convection probability forecast models for the cool (top), spring (center), and summer (bottom) season (see text for an explanation of the legend in the center panel).

Included in Fig. 2 are BSSs for separate SES convection probabilities, where these probabilities are geographically calibrated with regionalized regression equations (SES-REG; see section 4). Note that BSSs for SES-REG probabilities are consistently higher than those for the ("national") SES probabilities despite the relatively short developmental sample used [the samples used in the authors' previous regionalized gridded statistical forecast applications (CS; Charba and Samplatsky 2011b) were substantially longer]. Thus, the regional approach was considered (and ultimately used) for development of the LAMP convection probability regression equations (next section).

4. LAMP CONVECTION PROBABILITY FORECASTS

4.1 Regression Equation Development

With the LAMP approach, short range (30 hours and less) MOS convection probability forecasts issued four times per day are updated hourly through use of various observations-based predictors. The MOS updates come from LAMP convection probability regression equations, where the predictors consist of the GFS- and NAM-based convection probabilities, the GFS-NAM probability product, and various observations-based LAMP predictors. The latter are essentially identical to those used to produce currently operational lightning probability forecasts (Charba and Liang 2005a), except here the climatological monthly relative frequency of the convection predictand (an example of which is shown in Fig. 3) replaces a corresponding lightning climatology. (The high spatial coherency of the July relative frequencies in Fig. 3 results from smoothing raw frequencies computed from 1997 – 2010 historical data.) Also, radar-reflectivity-based variables have a stronger predictive role for the convection predictand than for the lightning predictand (not shown). This results from an internal correlation of the radar predictors with the convection predictand, as radar reflectivity data are used to specify both variables.

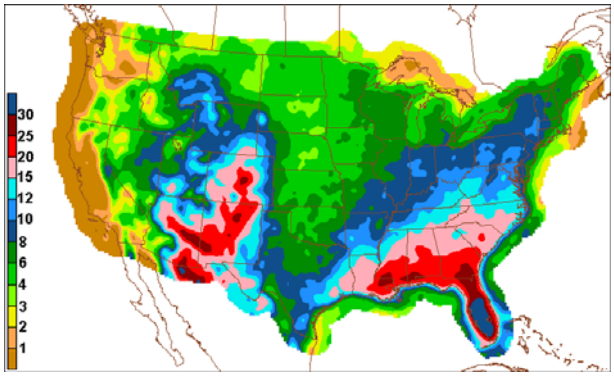

Figure 3. July relative frequency (%) of the convection predictand during 2200 – 0000 UTC.

As noted in the previous section, a geographically-regionalized approach was used for development and application of the LAMP convection probability regression equations. With this approach, the inevitable problem of inconsistency of the gridded convection probabilities across regional boundaries (CS; Charba and Samplatsky 2011b) required treatment. Following the work of Charba and Samplatsky, the treatment involves use of overlapping geographical regions in the development and application of the convection probability regression equations. The overlapping regions shown in Fig. 1 were used for each of the three seasonal stratifications of the LAMP regression equations (the LAMP seasonal stratification is the same as for MOS). It is noted that the overlapping-regions method described in CS is an earlier version of the method used by Charba and Samplatsky (2011b). This earlier version was not adopted here because it involves tedious tuning of complex smoothing procedures that are applied along the regional boundaries to mitigate regional discontinuities. The preferred Charba and Samplatsky method avoids boundary discontinuities altogether even for regions with relatively small overlap, e. g., regions 10 and 13 in Fig. 1. This is evident from the absence of regional discontinuities in example probability maps in section 5.

4.2 LAMP versus MOS Convection Probability Skill

Here, we examine the MOS updating performance of regionalized LAMP convection probabilities for the 1800 UTC LAMP cycle, whereby the GFS-NAM probabilities being updated are from the 1200 UTC cycle. Included in the performance comparison are LAMP convection probabilities based on non-regionalized (national) regression equations. Figure 4 shows seasonally-stratified BSSs for the regionalized (REG) and national (NAT) LAMP convection probabilities together with the MOS SES probabilities (discussed in section 3) for the same independent sample as for Fig. 2. Here we find REG skill is higher than SES skill at all LAMP projections to 24 hours for all three seasons. Also, REG skill improvement on SES is quite strong for LAMP forecast projections up to 6 hours, which reflects the important predictive role of “extrapolated” observations-based radar and lightning variables (see Charba and Liang 2005a). Another important finding is that REG skill is consistently higher than NAT skill. Further, REG skill improvement on NAT is rather substantial during the cool season for all projections, which may be attributed to the strong geographical variation in convection during that time of the year. Finally, NAT skill improvement on SES is marginal beyond 8 to 12 hours, depending on the season. This indicates REG skill improvement on SES at the long projections is due mainly to the regionalization. Thus, all subsequent references to LAMP convection probabilities involve geographical regionalization.

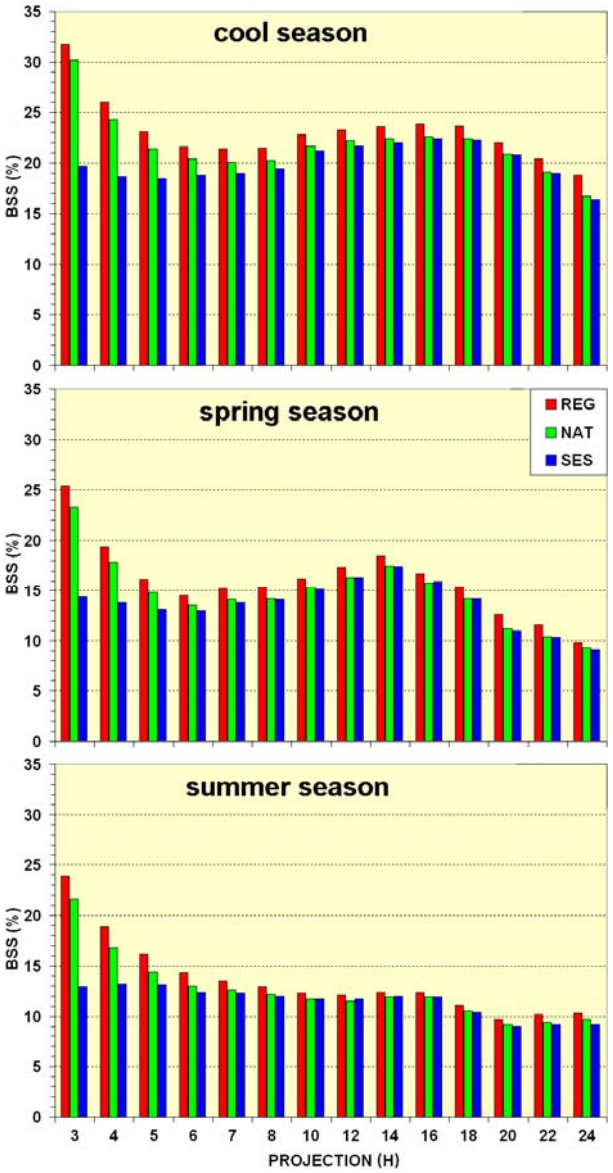

Figure 4. Seasonal BSS versus forecast projection (h) from 1800 UTC for regionalized (REG) and "national" (NAT; see text) LAMP convection probability forecasts. Included are BSSs for SES MOS probabilities from Fig. 2 (add 6 hours to LAMP forecast projections).

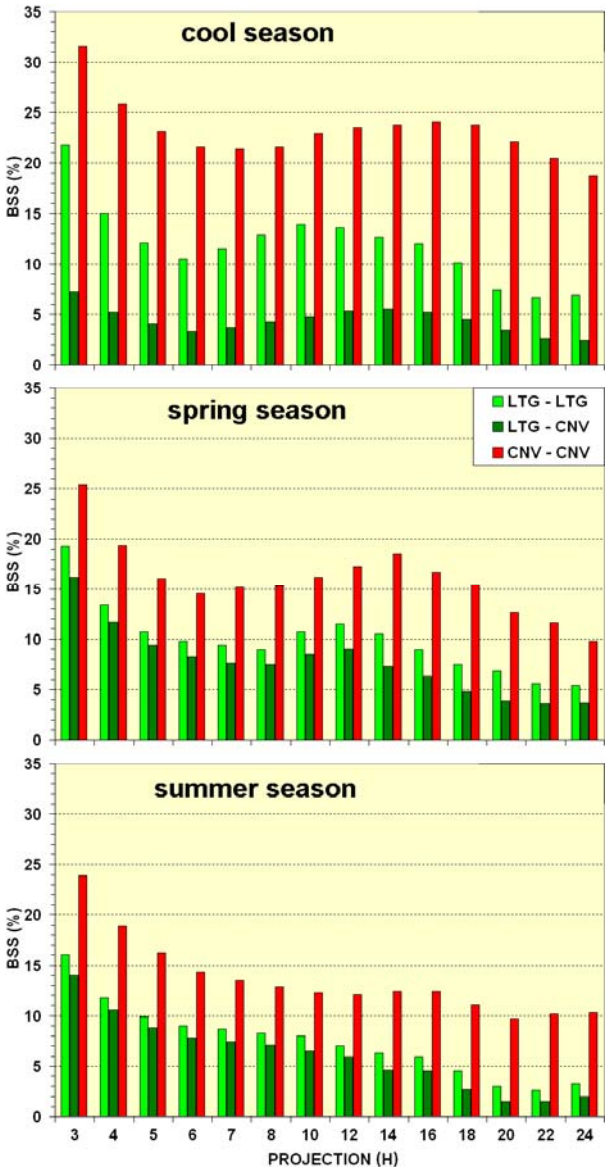

Figure 5. As in Fig. 4 for LAMP lightning and convection probabilities (see text for explanation of the legend). Note that BSSs for CNV-CNV and REG in Fig. 4 are identical.

4.3 LAMP Convection Probability versus Lightning Probability Skill

Since an important goal of this study was to improve the skill and sharpness of the current LAMP lightning probabilities (see Introduction; CS), here we investigate whether this goal was achieved. In Fig. 5, BSSs for LAMP lightning and convection probabilities are shown for the same cycle and sample as for Fig. 4. Here, the BSSs for the lightning probabilities are computed two ways: for the method denoted LTG-LTG the lightning probabilities are verified against the lightning predictand and climatology; for the method denoted LTG-CNV the lightning probabilities are verified with the convection predictand and climatology. For the convection probabilities the BSSs are computed only with the convection predictand and climatology; these BSSs are denoted CNV-CNV. Note that while a quantitative comparison of the BSSs for LTG-LTG versus CNV-CNV is not strictly valid (since the predictands are not identical) the comparison should be meaningful as the predictands are rather similar (section 3). Also, compar-

ing BSSs for LTG-CNV and CNV-CNV is valid, but it is unfair to score the lightning forecasts with the convection predictand. Still, these scores are meaningful because the lightning probabilities are being considered as a guidance tool for aviation planning and operations (Mahoney et al. 2009).

From Fig. 5 we find the CNV-CNV BSSs are about twice the LTG-LTG BSSs over the three seasons and all forecast projections. Also, the skill superiority of CNV-CNV is greater in the CNV-CNV versus LTG-CNV BSS comparison, which is expected for the reason given above. Interestingly, the skill superiority of CNV-CNV is huge during the cool season; it is smaller during the summer. Since precipitation is generally more electrified during summer than during winter, this finding may reflect a larger disparity in the lightning and convection predictands during the latter season. Another important feature in Fig. 5 is that the drop-off in skill with increasing forecast projection is substantially less for CNV-CNV than for LTG-LTG. This finding likely reflects the greater predictive contribution of the combined GFS-NAM MOS input in the convection model compared to the smaller GFS-MOS-only input in the lightning model. Note from Fig. 2 that the skill drop-off rate for the NWP models is rather gradual.

Mahoney et al. (2009) found that the LAMP 1500 UTC lightning probabilities during July - August 2009 were not useful as a supplement to the CCFP product (which is valid in the 2- to 6-h range); for longer ranges the utility of LAMP was no better. Thus, the above lightning versus convection BSS comparison is repeated for 1500 UTC during summer in Fig. 6. Again we find that the BSSs for CNV-CNV are about double those for LTG-LTG. Also, the skill drop-off with increasing projection is less for convection than for lightning, although not to the degree as for 1800 UTC (Fig. 5). Thus, the convection probabilities should provide improved forecast guidance for the aviation applications. Still, the summer season skill for both the convection and lightning probabilities at 1500 UTC is lower than for 1800 UTC. The skill degradation at 1500 UTC likely arises for two reasons: (1) the LAMP radar and lightning predictors are less effective at 1500 UTC, as this time generally precedes the initiation of the climatic diurnal convective peak; (2) the MOS input may be weaker at 1500 UTC than at 1800 UTC because it has increased latency (9 hours versus 6 hours, respectively) and it is based on an “off-time” (0600 UTC) NWP cycle rather than an “on-time” (1200 UTC) NWP cycle.

The reliability and sharpness are additional properties of probability forecasts that relate to their utility (Wilks 2006). These properties of the LAMP lightning and convection probabilities, for seasons, cycles, and forecast projections with contrasting skill, are shown in Fig. 7. We find the reliability for 1800 UTC convection probabilities during the cool season for a short projection [4-h, where the skill is relatively high (Fig. 5)] is generally good, as the forecast probability versus observed relative frequency curve hugs the perfect reliability line except for peak probability values. The reliability for this cycle and season is also good at the long (22-h) forecast projection. For 1500 UTC during summer the reliability for both the convection and lightning probabilities appears somewhat poorer for the 4-h projection.

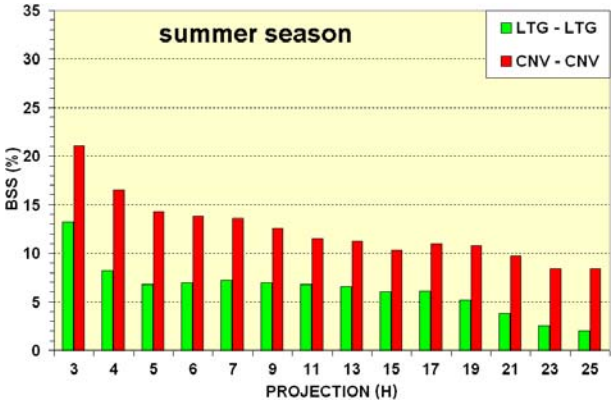

Figure 6. As in Fig. 5, except for the 1500 UTC cycle during the summer season and LTG-CNV is excluded.

A much greater contrast between the convection and lightning probabilities appears in the sharpness, as depicted in the probability distribution plots in Fig. 7. Note that the convection probabilities exhibit far better sharpness (many more cases of high probability values) than the lightning probabilities, especially at the long forecast projections (22-h projection at 1800 UTC and 21-h projection at 1500 UTC). Finally, note that the sharpness for the convection probabilities is somewhat better at 1800 UTC than at 1500 UTC for both the short and long projection. This is consistent with the increased skill at the former cycle (Figs. 5 and 6, respectively).

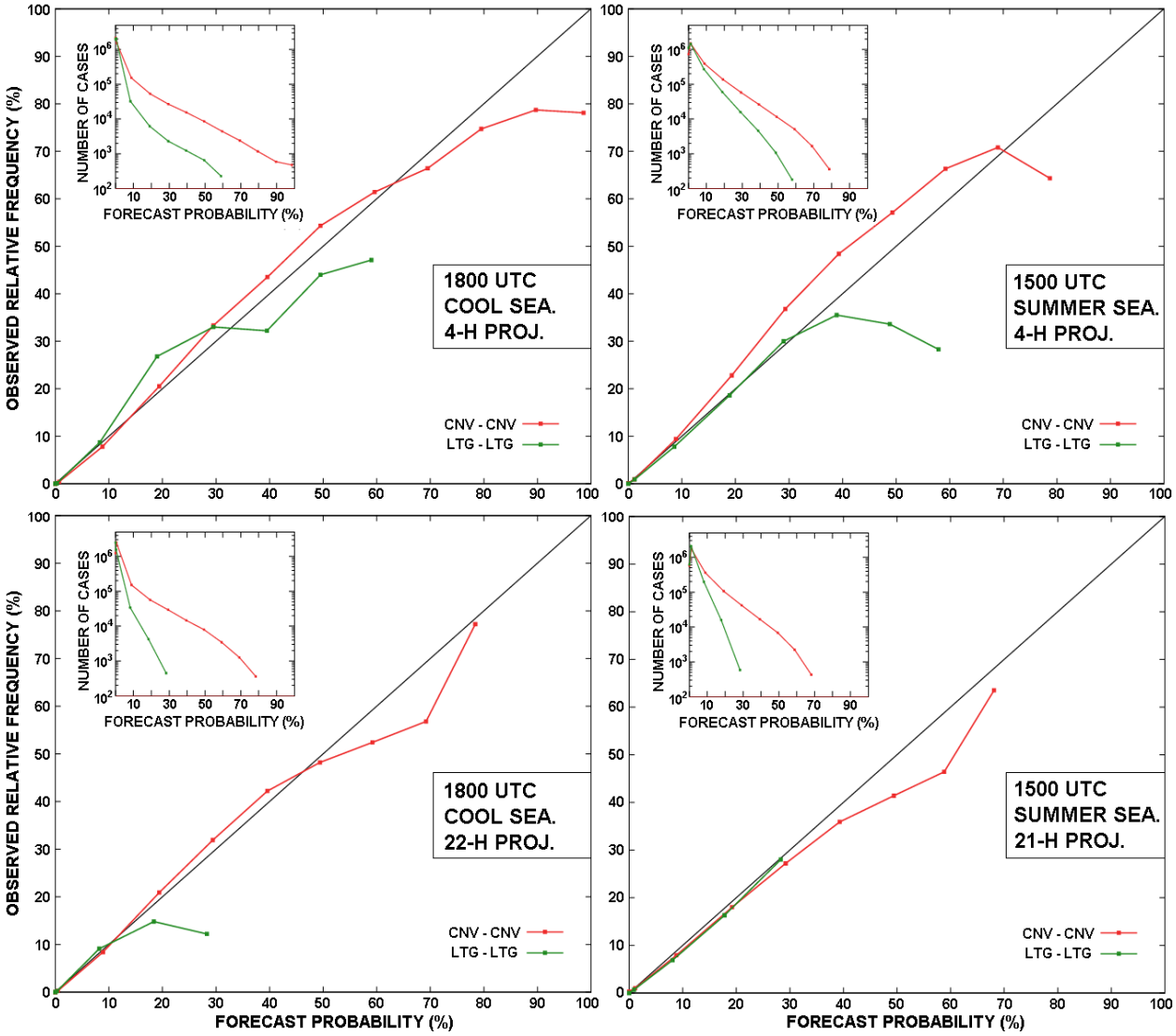

Figure 7. Reliability and frequency distribution (inset) of the LAMP lightning and convection probabilities for the 1800 UTC cycle during the cool season (left) and 1500 UTC cycle during the summer season (right). The ordinate scale in the frequency distribution charts is logarithmic. The legend is the same as in Figs. 5 and 6, and perfect reliability is indicated by the straight diagonal line in the reliability chart. The probability values plotted are means within 10 % probability intervals (5 % intervals near 0 and 100 %); means for (upper) probability intervals with less than 100 cases not plotted.

5. LAMP CONVECTION PROBABILITIES VERSUS LIGHTNING PROBABILITIES FOR SELECTED CASES

In this section we briefly examine maps of LAMP convection versus lightning probabilities for selected cases of strong convection outbreaks. The cases were taken from the 2010 summer season, where the probabilities are "independent" for both the convection and lightning predictands. For each case, convection and lightning probabilities are shown together with the verifying observations for each predictand. The primary purpose is to see if forecast performance findings in the previous section are evident in individual forecasts.

Figure 8 shows 18-h convection and lightning probabilities from 1800 UTC 21 July 2010 along with the verifying observations. We find that peak convection probabilities are far higher than peak lightning probabilities, especially for the intense maximum in northern Iowa. Note that the Iowa convection probability maximum coincides with a solid area of observed convection; the lightning probabilities and observations also match well in this location. Also, the finding (in the previous sec-

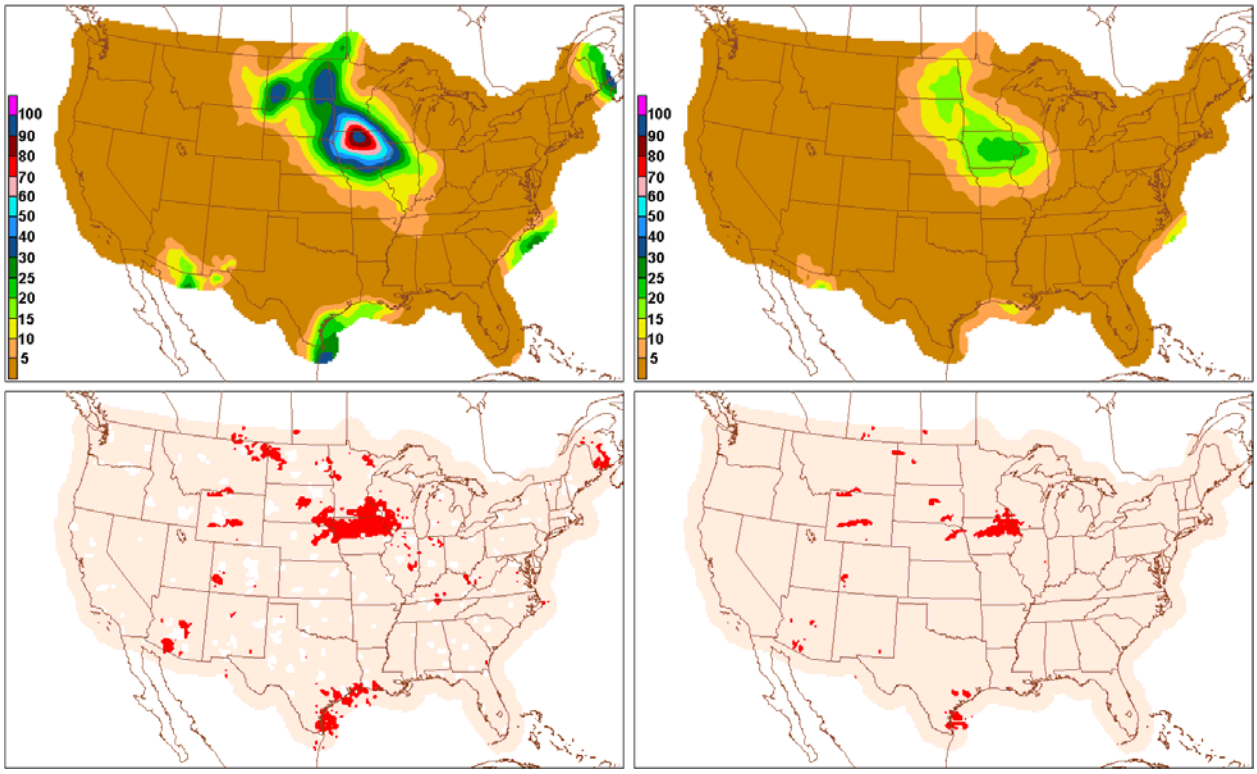

Figure 8. 18-h LAMP convection probability forecast (%; upper left) and verifying "yes/no" occurrences (lower left; red/pink) from 1800 UTC 21 July 2010. The corresponding lightning probabilities and verifying "yes/no" occurrences are to the right. The small white spots in the observed convection map indicate missing data, which results from quality control of the radar reflectivity data used (in part) to specify the convection predictand (see section 2).

tion) of superior sharpness of the convection probabilities is strikingly evident in this case.

Figure 9, which shows 6-h convection and lightning probabilities from 1800 UTC 12 August 2010, also reveals general similarity in the two forecast patterns. It is noted that for a relatively short forecast projection, such as we have here, high similarity in the convection and lightning forecasts is expected since LAMP radar and lightning predictors are heavily used for both predictands. Still, a major difference in the convection and lightning probabilities appears in this case along the Ohio-Pennsylvania border, where a strong peak in the convection probabilities coincides with a flat field of quite low probabilities in the lightning map. It is remarkable that each forecast verified quite well in this area, as a solid area of convection was associated with very little CTG lightning there. In fact, our examination of many cases has revealed that this situation is not rare. Also note that this finding underscores the statement in the previous section that it is inherently inappropriate to verify the lightning probabilities with the convection observations.

The final example shows 12-h forecasts from 1800 UTC 29 September 2010 (Fig. 10), where record setting torrential rain occurred with the remnants of Tropical Storm Nicole from South Carolina to Virginia. We find that the convection and lightning probabilities are strikingly different in this area, as peak convection probabilities exceeded 90% while corresponding lightning probabilities were only about 10%. Interestingly, the verifying maps show extensive convection but very limited CTG lightning there. While low lightning probabilities and scarce CTG lightning may be surprising for a heavy convection episode like this, we have noted such a situation for many tropical-system cases in our LAMP lightning prediction work (a good example is shown in Fig. 6 of CS).

Finally, note that each of the latter two cases contains the combination of high convection probability and low lightning probability where each forecast matched up well with the verifying observations. This suggests the convection and lightning forecasts could be used in a complementary manner to help identify these distinct convection episodes. The identification of these events

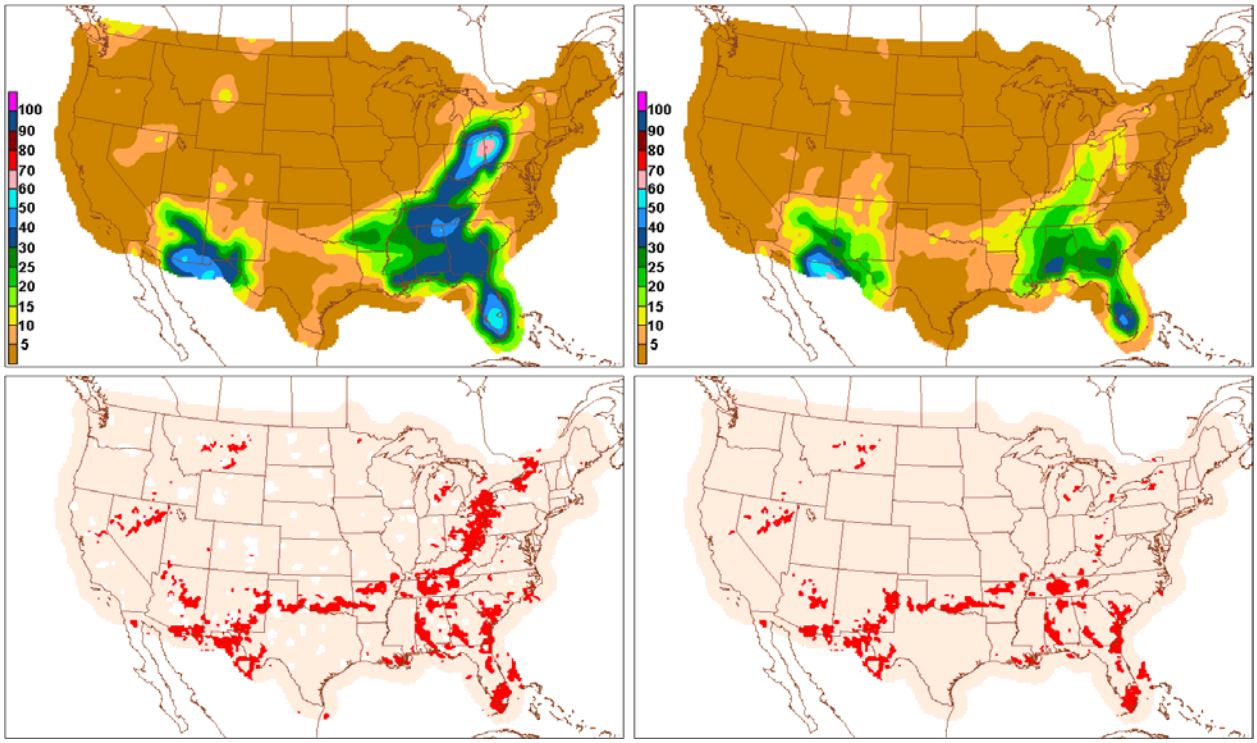

Figure 9. As in Fig. 8, except 6-h forecasts from 1800 UTC 21 August 2010.

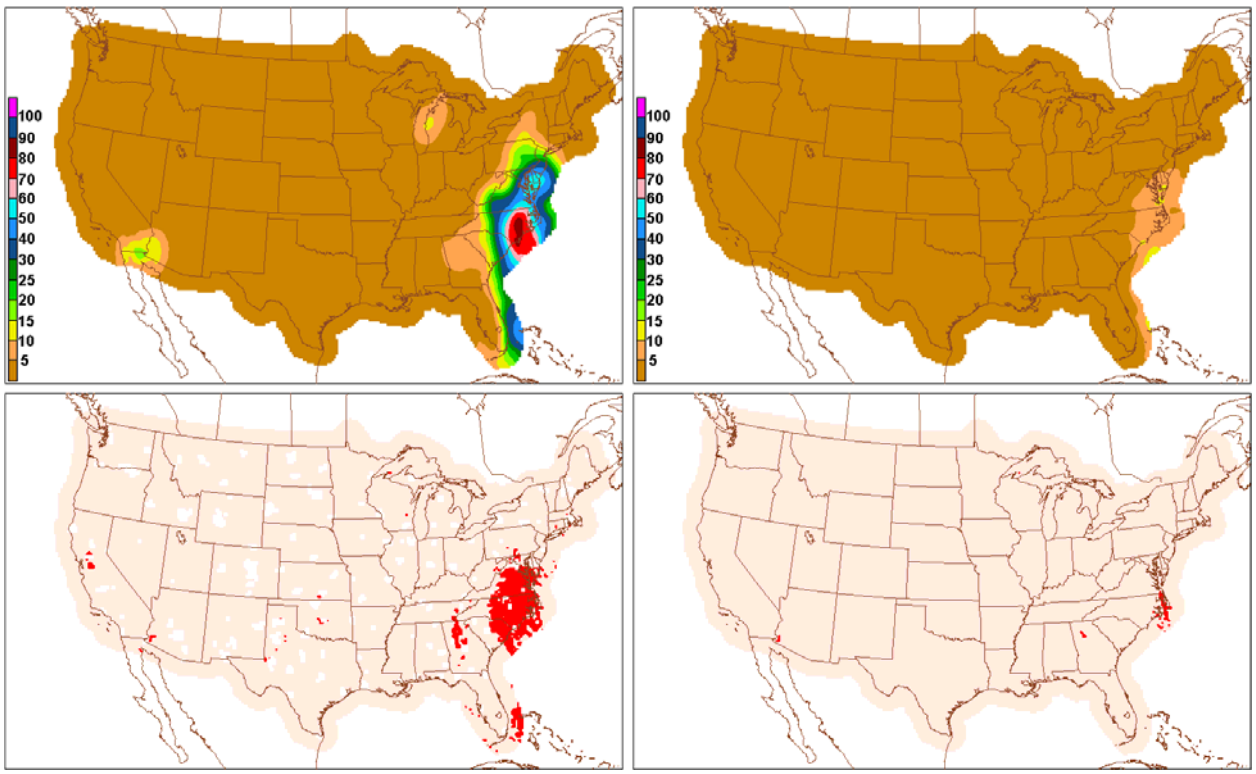

Figure 10. As in Fig. 8, except 12-h forecasts from 1800 UTC 29 September 2010.

should be quite valuable since convection with little or no lightning generally poses a far less hazard than highly electrified convection.

6. FINDINGS, CONCLUSIONS, AND PLANS

This study yielded the following findings:

(1) The LAMP convection predictand may be more suitable than the LAMP CTG lightning predictand for aviation applications;

(2) The combined use of the GFS and NAM model output to produce the MOS convection forecast input into LAMP was quite effective despite a relatively short NAM developmental sample (Fig. 2);

(3) The use of the GFS-NAM convection probability product as a supplemental predictor resulted in enhanced skill of the ensemble MOS convection probabilities (Fig. 2). This MOS enhancement is incorporated into LAMP;

(4) The application of geographical regionalization in the LAMP model development was beneficial despite the relatively short developmental sample used (Fig. 4);

(5) The skill of the LAMP convection probabilities was higher than that for the input MOS convection probabilities, especially at the shortest projections (Fig. 4);

(6) The skill of LAMP convection probabilities was much higher than that for operational LAMP lightning probabilities at all projections (Figs. 5 and 6);

(7) The sharpness of the LAMP convection probabilities was far better than the sharpness of LAMP lightning probabilities (Figs. 7 - 10);

(8) The LAMP convection and lightning probabilities complemented one another in two of three cases examined (Figs. 9 and 10).

Thus, we conclude that the LAMP convection probabilities (when implemented) should provide useful forecast guidance in applications where convection occurrences are defined from a combination of radar reflectivity and CTG lightning data. Also, the complementary use of LAMP convection probabilities and currently operational LAMP lightning probabilities could aid predicting the degree of CTG lightning activity in convection events. Tentatively, we plan to implement the LAMP convection probability and categorical (not discussed) forecasts for at least four cycles on an experimental basis in June 2011.

7. ACKNOWLEDGEMENTS

As leader of the LAMP program at MDL, Judy Ghirardelli provided general guidance and support of this work. Also, staff of the MDL Statistical Modeling Branch led by Kathryn Gilbert furnished most of the archived data that were used.

8. REFERENCES

Brier, G. W., 1950: Verification of forecasts expressed in terms of probability. *Mon. Wea. Rev.*, **78**, 1-3.

Charba, J. P., and F. Liang, 2005a: Automated two-hour thunderstorm guidance forecasts. Preprints*, Conference on Meteorological Applications of Lightning Data.* San Diego, Amer. Meteor. Soc., CD-ROM, **3.4**.

____, and ___, 2005b: Quality Control of gridded national radar reflectivity data. *21st Conf. on Weather Analysis and Forecasting*. Washington DC, Amer. Meteor. Soc., CD-ROM **6A.5**.

____, and F. G. Samplatsky, 2009: Operational 2-h thunderstorm guidance forecasts to 24 hours on a 2-km grid. Preprints, *23rd Conference on Weather Analysis and Forecasting/19th Conference on Numerical Weather Prediction*, Omaha, NE, Amer. Meteor. Soc., **15B.5**.

___, and ___, 2011a: High resolution GFS-based MOS quantitative precipitation forecasts on a 4-km grid. *Mon. Wea. Rev.*, **139**, 39-68.

___, and ___, 2011b: Regionalization in fine-grid GFS MOS 6-h quantitative precipitation forecasts. *Mon. Wea. Rev.*, **139**, 24-38.

Cummins, K. L., M. J. Murphy, E. A. Bardo, W. L. Hiscox, R. B. Pyle, and A. E. Pifer, 1998. A combined TOA/MDF technology upgrade of the U. S. national lightning detection network, *J. Geophys. Res.*, **103**, 9035-9044.

Fulton, R. A, J. P. Breidenbach, D. J. Seo, D. A. Miller, and T. O'Bannon, 1998: The WSR-88D rainfall algorithm. *Wea. Forecasting*, **13**, 377-395.

Ghirardelli, J. E., and B. Glahn, 2010: The Meteorological Development Laboratory's Aviation Weather Prediction System. *Wea. Forecasting*, **25**, 1027-1051.

Glahn, H. R., and D. A. Lowry, 1972: The use of model output statistics (MOS) in objective weather forecasting. *J. Appl. Meteor*., **11**, 1203–1211.

Hughes, K. K., 2004: Probabilistic lightning forecast guidance for aviation. Preprints, *22th Conference on Severe Local Storms,* Hyannis, MA, Amer. Meteor. Soc., CD-ROM **2.6**.

Kanamitsu, M., J. C. Alpert, K. A. Campana, P. M. Caplan, D. G. Deaven, M. Iredell, B. Katz, H. – L. Pan, J. Sela, G. H. White, 1991: Recent changes implemented into the Global Forecast System at NMC. *Wea. Forecasting*, **6**, 425-435.

Kitzmiller, D. H., F. G. Samplatsky, and D. L. Keller, 2002: Production of a national radar reflectivity mosaic and automated radar observations from WSR-88D radar coded messages. *NOAA Tech. Memo.* NWS MDL 83, National Oceanic and Atmospheric Administration, U.S. Department of Commerce, 23 pp.

Mahoney, J., S. Madine, S. Lack, and G. Layne, 2009: Assessment of the CCFP/LAMP Thunderstorm Hybrid product. Technical document prepared by the U.S. Department of Commerce, National Oceanic and Atmospheric Administration, Earth System Research Laboratory, Global Systems Division, 51 pp. (Available from Earth System Research Laboratory, NOAA, R/GSD5, 325 Broadway, Boulder, CO 80305-3328).

OFCM, 1991: Doppler radar meteorological observations: Part C, WSR-88D products and algorithms. Federal Meteorological Handbook 11, FMC-H11C-1991, Office of the Federal Coordinator for Meteorological Services and Supporting Research, Silver Spring, MD, 210 pp.

Rodgers, E., Y. Lin, K. Mitchell, W.-S Wu, B. Ferrier, G. Gayno, M. Pondeca, M. Pyle, V. Wong, and M. Ek, 2005: The NCEP North American-Mesoscale Modelling System: Final Eta model/analysis changes and preliminary experiments using the WRF-NMM. Preprints, *21st Conf. on Wea. Analysis and Forecasting*, Washington, D.C., Amer. Meteor. Soc., **4B.5**.

Wilks, D. S., 2006: *Statistical Methods in the Atmospheric Sciences.* 2nd ed. Academic Press, 627 pp.